

Integration of Different Density UAV Lidar and Single Beam Echo Sounder (SBES) for River and Riparian Area Digital Terrain Model (DTM) Construction

Puven Raj P. Chazian¹, Muhammad Zulkarnain Abd. Rahman^{1*}, Wan Hazli Wan Kadir¹, Azman Ariffin¹, Husaini Suhaili²

¹Geoinformation Program, Faculty of Build Environment and Surveying, Universiti Teknologi Malaysia, 81310 Johor Bahru, Johor, Malaysia

²Perunding Geomatik Sdn. Bhd., Lot1998 Marina Parkcity 2, 98000 Miri, Sarawak, Malaysia

*Corresponding author: mdzulkarnain@utm.my

Abstract - Rivers and riparian areas are vital components of ecosystems, but accurately modeling their terrain presents challenges, especially in detecting the river surface. This paper proposes an integrated approach that combines UAV LiDAR and Single Beam Echo Sounder (SBES) data to construct a Digital Terrain Model (DTM) of river and riparian areas. The objective is to overcome the limitations posed by water, which absorbs near-infrared laser energy, resulting in weak or absent LiDAR returns. Different UAV LiDAR densities were examined to determine the optimal configuration for capturing riparian areas. Evaluation of the results utilized various metrics, including root mean square error (RMSE), mean square error (MSE), mean absolute error (MAE), mean bias error (MBE), and correlation coefficient (CC). Three ground filtering methods were implemented and assessed: morphological filters, adaptive triangulated irregular network (ATIN) filtering, and above-ground level (AGL) filtering. Among the evaluated methods, the DTM constructed using ATIN with an 80-meter flight configuration yielded the most accurate results. It achieved an RMSE of 0.18m, an MSE of 0.03m, an MAE of 0.17m, an MBE of 9.08m, and a CC of 1.00. Comparatively, other methods exhibited higher error values and lower correlation coefficients. The findings highlight the efficacy of ATIN filtering in conjunction with an 80-meter UAV LiDAR flight for obtaining reliable DTMs of river and riparian areas. This approach demonstrates significant improvement in accuracy, particularly in terms of RMSE and MSE. The derived DTM can be a valuable tool for safeguarding and managing these critical ecosystems. In summary, this paper successfully addresses the challenge of modeling river and riparian terrains by integrating UAV LiDAR and SBES data. By employing ATIN filtering with an 80-meter flight configuration, the study achieves a highly accurate DTM. By employing ATIN filtering with an 80-meter flight configuration, the study achieves a precise, high DTM with minimal error. The developed model contributes to protecting and preserving river and riparian ecosystems.

Keywords – *Light Detection and Ranging (LiDAR), Single Beam Echo Sounder (SBES), Digital Terrain Model (DTM), and Adaptive Triangulated Irregular Network (ATIN)*

©2024 Penerbit UTM Press. All rights reserved.

Article History: Received 1 February 2024, Accepted 25 February 2024, Published 31 March 2024

How to cite: Chazian, P. R. P., Abd. Rahman, Z., Wan Kadir, W. H., Ariffin, A. and Suhaili, H. (2024). Integration of Different Density UAV LiDAR and Single Beam Echo Sounder (SBES) for River and Riparian Area Digital Terrain Model (DTM) Construction. Journal of Advanced Geospatial Science and Technology. 4(1), 106-129.

1.0 Introduction

The construction of Digital Terrain Models (DTM) for river and riparian areas is important for various applications such as flood risk assessment, river channel maintenance, erosion analysis and habitat restoration (Akihisa et al., 2011). However, obtaining accurate and detailed DTMs for these areas is challenging due to the complex topography and vegetation cover (Nedjati et al., 2015). One such area is the Seblak River in Sarawak, Malaysia, where the water is known to be cloudy, and the river is affected by tides, making it difficult to obtain accurate topographic information on the riverbed using traditional methods such as ground-based surveying and photogrammetry (Lin et al., 2011).

Recent advancements in Unmanned Aerial Vehicle (UAV) technology have revolutionized DTM construction by facilitating the acquisition of high-resolution topographic data in previously inaccessible areas. Among the various UAV-based techniques, UAV Lidar stands out for its ability to deliver high-resolution datasets even with low point density, making it a preferred choice for DTM construction (Meng et al., 2010). However, despite its prowess, UAV Lidar alone may not adequately capture the intricate topography of rivers and riparian zones, especially in regions characterized by dense vegetation, murky water, and tidal influences (Nedjati et al., 2015).

One technique that complements UAV Lidar is the Single Beam Echo Sounder (SBES), renowned for its capability to map riverbeds and riparian areas meticulously. SBES emits a single sound beam to measure water depth, providing invaluable insights into the underwater landscape, including detecting features like sandbars and gravel bars (Akihisa et al., 2011). However, challenges arise in environments like the Seblak River, where cloudy water and tidal effects can compromise the accuracy of SBES data due to issues such as turbidity, signal attenuation, and interference.

Recognizing the complementary strengths and limitations of UAV Lidar and SBES, their integration offers a compelling solution for mapping riparian areas with enhanced accuracy and detail (Meng et al., 2010). Combining UAV Lidar's prowess in capturing terrestrial topography with SBES's proficiency in mapping underwater features can better understand the riverbed morphology and riparian landscape (Zhang et al., 2020). This integrated approach identifies intricate features that may elude detection by either technique alone.

Pre-processing steps such as above-ground filtering (AGL) are required to enable accurate terrain information. AGL is a technique for isolating specific elements from lidar data, such as buildings, vegetation, and other above-ground features. Its purpose is to distinguish the ground surface from objects (Axelsson, 2000). Triangulated Irregular Network (TIN) is a

popular DTM creation method from point cloud data, particularly for natural terrain and hydrological applications. This method creates a triangular network of points, connecting each point to its nearest neighbours. This creates a smooth surface that represents the terrain and allows for the generation of contours and other derived products. TIN is beneficial for handling large datasets and creating DTMs in steep or rugged terrain (Meng et al., 2010). However, TIN can make a surface that is too smooth, losing fine-scale details and small features such as small islands and channels in the riverbed (Hudson & Harrison, 2016).

Morphological filtering is another method to filter point clouds to remove noise and outliers (Meng et al., 2010). This method uses mathematical morphology operations, such as erosion and dilation, to identify and remove points that do not belong to the terrain surface (Zhang et al., 2020). Morphological filtering can help remove vegetation, buildings, and other non-terrain features from the point cloud data. It can also filter out noise and outliers caused by measurement errors or other factors. However, it can also remove important features, such as small islands and channels in the riverbed, primarily when aggressive filtering is used (Zhang et al., 2020).

DTM generation algorithms have partially replaced human interpolation and become a post-processing step after the data acquisition from these remote sensing systems. According to Maguya *et al.* (2014), this phase is usually divided into classification and interpolation. The classification step extracts the bare earth information (such as elevation, intensity, multiple-returns, or some calculated features like average vector segments) from the acquired data, automatically classifying the gathered data into terrain and off-terrain. This process is known as “filtering” in the airborne laser scanning community. Subsequently, the DTM can be generated by interpolating the extracted terrain data (Maguya et al., 2014).

Several methods have been proposed to assess the quality of DTMs. Root mean square error (RMSE) and mean signed error (MSE) are commonly used statistical measures for evaluating DTM accuracy. Previous research extensively relies on RMSE to gauge the accuracy of DTMs derived from remote sensing techniques like Lidar and photogrammetry. A lower RMSE value indicates a more substantial alignment between predicted and reference values, signifying higher accuracy. Similarly, MSE serves as another crucial metric, measuring the average disparity between predicted and reference DTM values. This measure is valuable for comparing different filtering or processing techniques, highlighting their effectiveness in minimizing DTM errors.

Meanwhile, mean absolute error (MAE) is often employed alongside RMSE and MSE to offer comprehensive insight into DTM accuracy and precision. MAE complements RMSE

by capturing the average error magnitude, with lower values indicating higher accuracy and agreement. Mean bias error (MBE), or mean error (ME), provides insights into the systematic bias of a DTM, indicating whether it consistently overestimates or underestimates ground elevation. Lastly, the correlation coefficient (CC) evaluates the linear relationship between predicted and reference DTM values. By quantifying the strength and direction of this correlation, CC offers valuable insights into the consistency and reliability of the DTM. These measures collectively contribute to a robust assessment of DTM quality, aiding in informed decision-making and interpretation of terrain data.

The study aims to acquire LiDAR and SBES data at various densities over the Seblak River in Sarawak. It intends to construct DTM using a combination of UAV LiDAR data of different densities, SBES data, and various LiDAR ground filtering methods. The evaluation of the DTMs will be based on ground checkpoints.

2.0 Material and Methods

The study area in Kampung Sungai Benang, Daerah Kabong, Bahagian Betong, Sarawak, Malaysia, is known for its peat swamp forest and brackish river water (Figure 1). The size of the study area is 2 km². The number of ground checkpoints is 36. As noted in a previous study, the Seblak River is characterized by cloudy water and an active riparian zone.

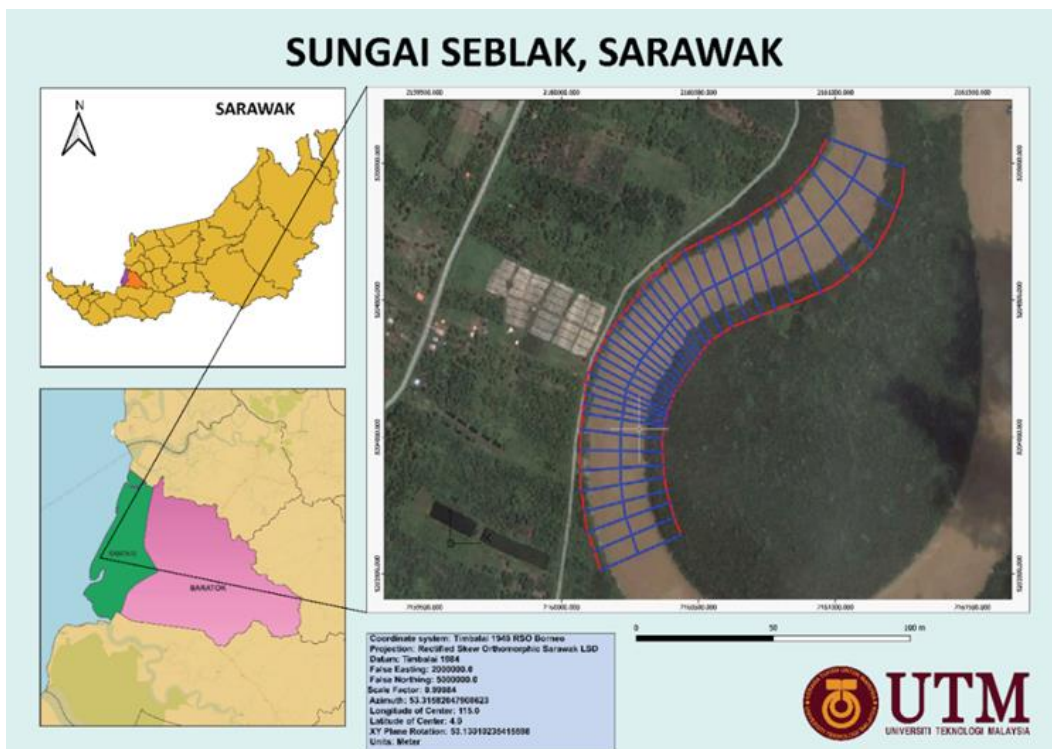


Figure Error! No text of specified style in document.. Location of study area

2.1 Flowchart

The methodology of this study comprises three primary phases: data acquisition, DTM construction and analysis, and accuracy assessment. In the data acquisition phase, various density UAV LiDAR and SBES data are collected from the study area in Kampung Sungai Benang, Daerah Kabong, Bahagian Betong, Sarawak, Malaysia. Subsequently, in the DTM construction and analysis phase, the acquired data undergoes processing and integration utilizing different LiDAR ground filtering methods, such as TIN and morphological filtering, to produce the DTM. This phase involves intricate data manipulation and combination techniques to represent the terrain comprehensively.

Finally, the accuracy assessment phase involves the evaluation of the generated DTM using ground checkpoints. These checkpoints serve as reference data to validate the accuracy and reliability of the DTM. The methodology flowchart, depicted in Figure 2, delineates the step-by-step workflow of the research methodology.

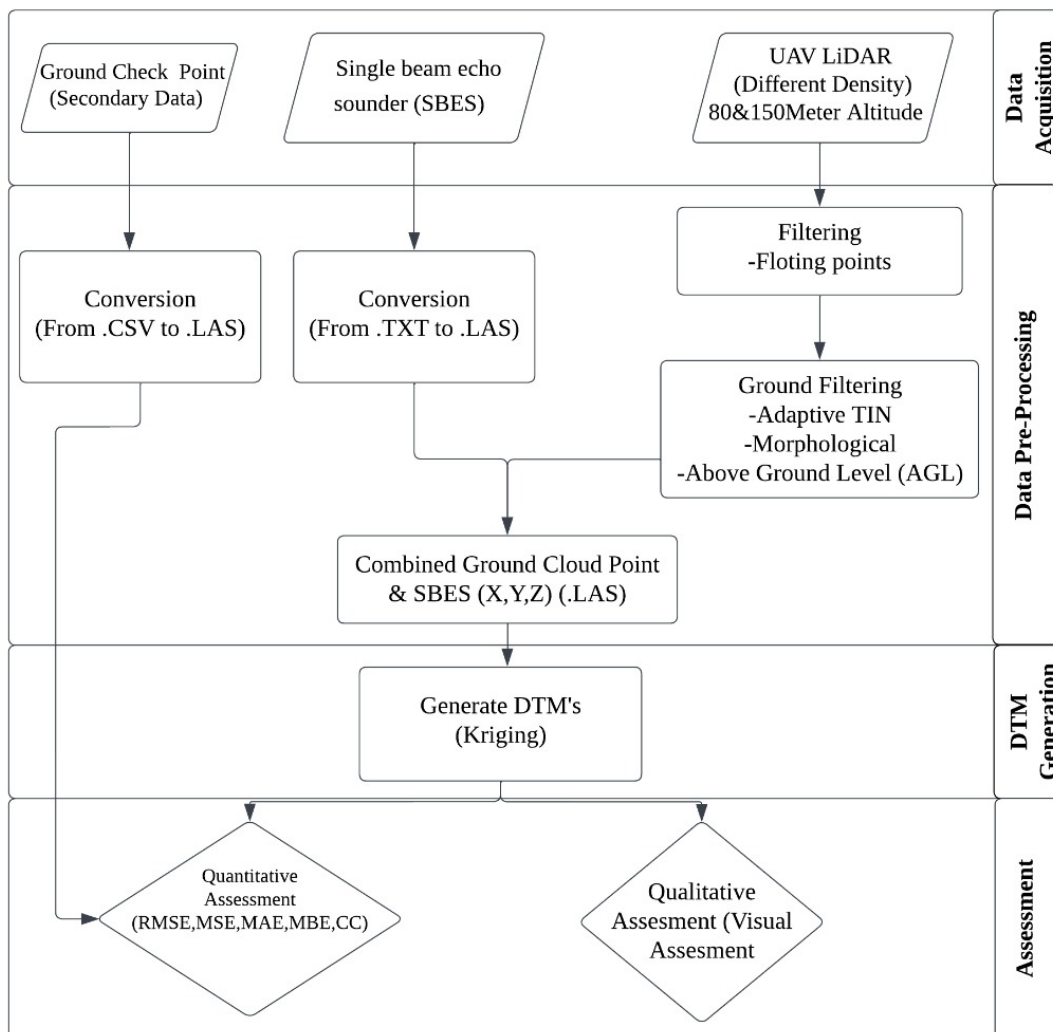


Figure 2. Research methodology flowchart

2.2 Data Acquisition (Phase 1)

Data acquisition is important in constructing an accurate DTM. Two methods, UAV Lidar and SBES, were utilized for data collection. The UAV Lidar data was acquired using a DJI Matrice 600 Pro (Figure 3) and a gAirHawk Air Eagle GS-260S (Figure 4), equipped with high-resolution LiDAR sensors capable of capturing dense point clouds. These UAV systems offered versatility in various environmental conditions, including challenging scenarios like cloudy water bodies.

For SBES data collection, CHC D390 Side Mounted Units (Figure 5) and CHC D390 topside (Figure 6) were employed. These systems were specifically designed for shallow waters and provided high-resolution data with a dense point density, ensuring precise measurements. A GNSS Receiver (SATLAB SL700) (Figure 7) was utilized for multiple purposes, including collecting ground checkpoints for accuracy assessment and serving as a base GNSS RTK for the LiDAR and SBES systems. A total of 3240 SBES data were collected and used.

The study area's topography was comprehensively understood by integrating data from UAV LiDAR, SBES, and the GNSS Receiver. The data collection phase was completed on March 23, 2023, during which data was acquired using the specified instruments and techniques. Subsequently, the collected data was utilized to construct the DTM of the study area, ensuring a detailed representation of its topographic features. A total of 7,971,133 LiDAR point clouds were collected using this system.



Figure 3. DJI Matrice 600 Pro



Figure 4. gAirHawk Air Eagle GS-260S



Figure 5. CHC D390 Side Mounted Units



Figure 6. CHC D390 topside



Figure 7. GNSS Receiver (SATLAB SL700)

2.2 Pre-Processing (Phase 2)

Data pre-processing encompasses several essential steps to prepare the collected SBES and ground checkpoint data for integration and analysis. The initial stage involves converting the existing SBES and ground checkpoint data formats into a standardized format compatible with other project data, such as .las files. This conversion can be efficiently performed using Microsoft Excel by uploading the raw SBES data in .CSV format and saving the file in the desired format.

For the UAV Lidar data, pre-processing entails the removal of floating points within the point clouds. Often regarded as error points, these points do not correspond to any features in the real world and can adversely affect data accuracy. In this project, several hundred floating points were identified and eliminated before proceeding to subsequent processing steps (Figure 8). There is a total of 215,734 floating points, and they were removed.

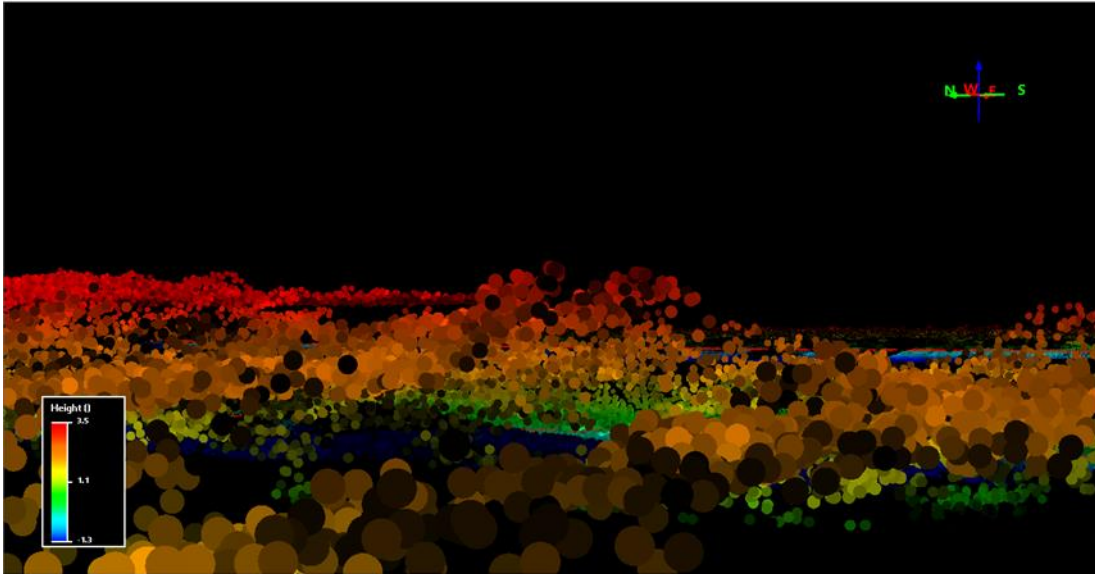


Figure 8: Removing floating points

After the initial removal of floating points, the pre-processing of Lidar data continues with more specific filtering methods, mainly targeting the extraction of ground points. This study's objective includes exploring various ground filtering techniques, including adaptive TIN (ATIN), morphological filtering, and AGL filtering.

The ATF (ATIN) technique utilized a TIN algorithm and a morphological filter to selectively eliminate outliers and noise from the Lidar point cloud data. Initially, the TIN algorithm triangulates the point cloud data, creating a mesh of irregular triangles representing the terrain surface. Subsequently, the morphological filter is applied to identify and remove outliers and noise based on the slope and height characteristics of the terrain (Figure 9).

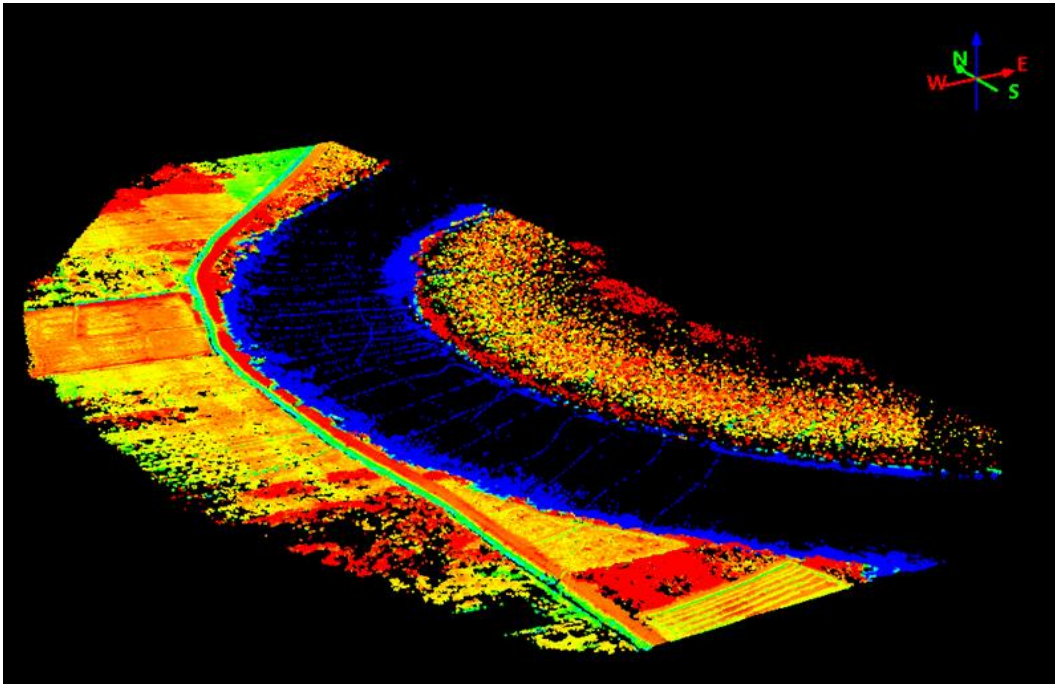


Figure 9. ATIN-filtered UAV Lidar data

A morphological filter technique and free, open-source software, ALDPAT, were used to filter the ground. There are five filtering techniques provided by ALDPAT: Elevation Threshold with Expand Window (ETEWE), Morphological, Slope, Polynomial, and Adaptive TIN filter (Figure 10).

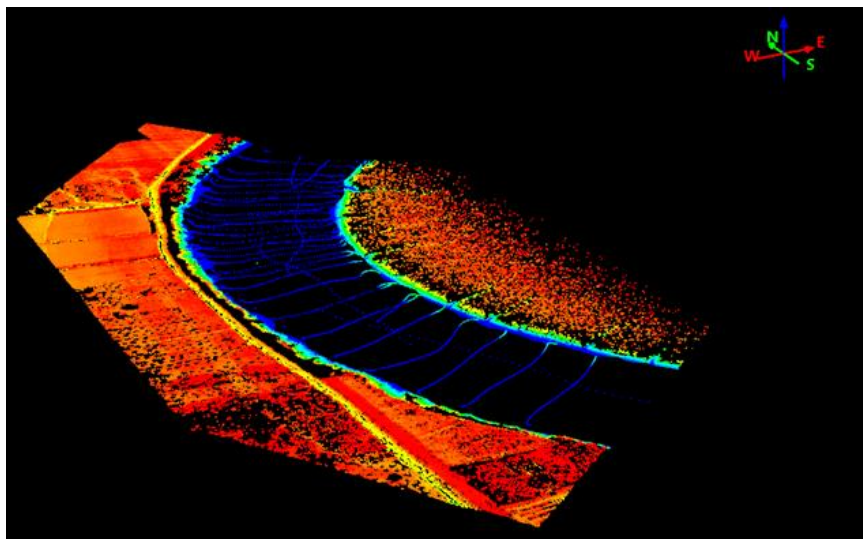


Figure 10. Morphologically filtered ground data

AGL filtering is a crucial step in the data processing workflow, aiming to remove non-ground objects and retain the ground surface information in the DTM (Figure 11). This

subsection explains the AGL filtering process in-depth, including determining the threshold value and its implications for DTM accuracy.

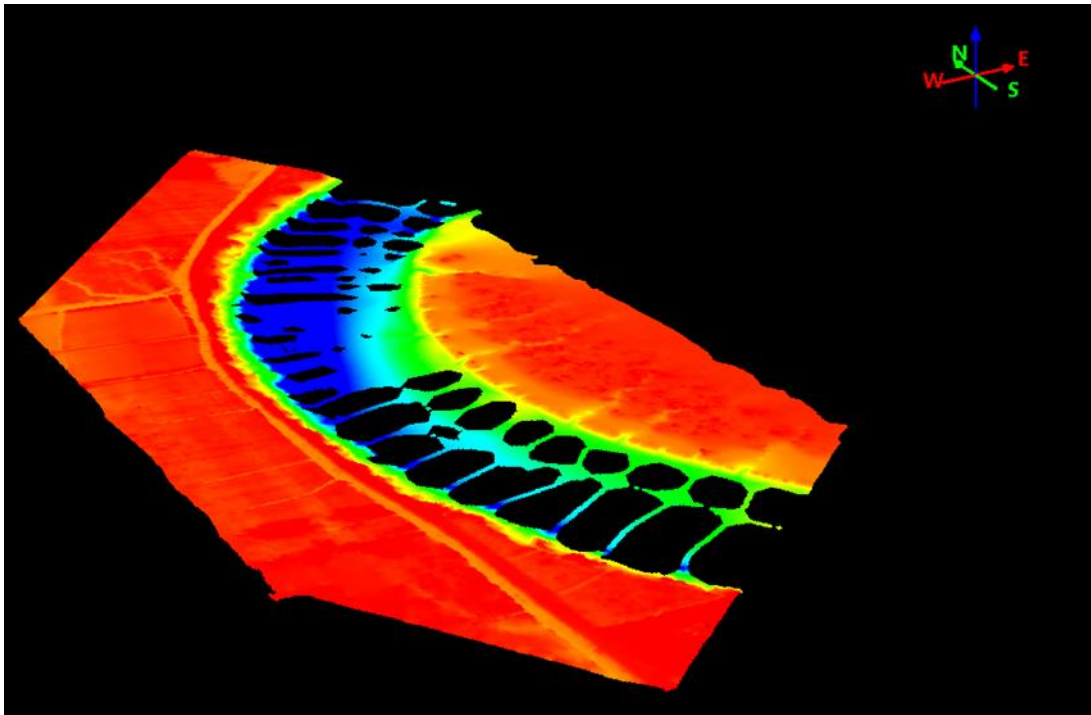


Figure 11. AGL filtered data

The last pre-processing step is combining point clouds. The point clouds obtained from the UAV Lidar and SBES data will be combined to create a comprehensive DTM for the study area (Figure 12). This process involves merging the point clouds from the two data sources into a single point cloud. This is done by aligning the point clouds using common points and a registration algorithm to ensure that the point clouds are accurately aligned. Once the point clouds are aligned, they are combined to form a single point cloud representing the entire study area.

Table 1 provides information on the number of point cloud data points at different processing stages after applying various filtering methods: ATIN, AGL filtering, and morphological filtering. Initially, over 7 million data points were collected. However, after filtering, about 3 million cloud data points remain for each filtering method.

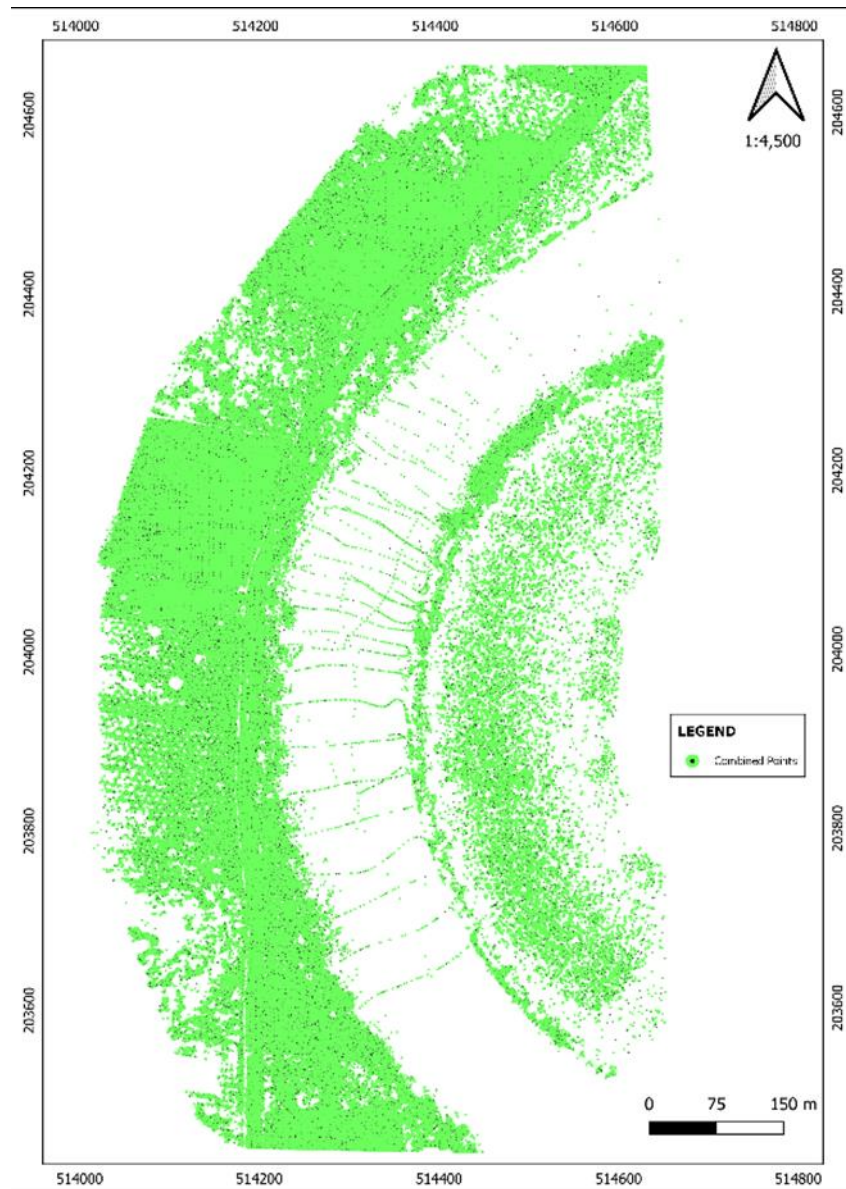


Figure 12. Combining ground-filtered UAV Lidar and SBES data

Table 1. Number of point clouds after filtering

| Point Cloud | ATIN | AGL | Morphological filter |
|-----------------------|-------------|------------|-----------------------------|
| RAW | 7,971,133 | 7,971,133 | 7,971,133 |
| Pre-Processing | 7,755,399 | 7,755,399 | 7,755,399 |
| Filtering | 3,458,772 | 3,165,739 | 3,345,629 |

2.3 DTM Generation (Phase 3)

Generation of a digital terrain model (DTM) is one of the main steps in this study. The DTM is generated using SURFER software. The interpolation method used for generating the DTM is kriging, and the pixel size of the DTM is 1 meter. This step is repeated six times for all, and six generated DTMs were used for this study.

2.4 Accuracy Assessment (Phase 4)

2.4.1 Quantitative analysis

Quantitative analysis plays a crucial role in this study, enabling the evaluation of the accuracy of the generated DTM. Five quantitative analysis methods were employed, including calculating RMSE, MSE, MAE, MBE, and CC. These metrics provide valuable insights into the vertical accuracy of the DTM by comparing it with the ground truth measurements obtained from the ground checkpoints. A total of 36 ground checkpoints were used in this quantitative assessment.

RMSE is a widely used metric for quantifying the overall discrepancy between the elevations obtained from the DTM and the ground checkpoints. It measures the average magnitude of the differences in the z-coordinate values. The RMSE calculation formula is as follows:

$$RMSE = \sqrt{\frac{\sum(DTM - Ground)^2}{n}}$$

MSE is a metric that quantifies the average squared differences between the DTM elevations and the ground checkpoints. It measures the overall error magnitude, capturing both systematic and random errors. The MSE calculation formula is as follows:

$$MSE = \frac{(\sum(DTM - Ground)^2)}{n}$$

Both RMSE and MSE assess the overall accuracy and goodness-of-fit of the DTM.

MAE is a metric that calculates the average absolute differences between the DTM elevations and the ground checkpoints. It provides insights into the average magnitude of the errors, irrespective of their direction. The MAE calculation formula is as follows:

$$MAE = \frac{(\sum |DTM - Ground|)}{n}$$

By calculating MAE, the average absolute deviation between the DTM and the ground truth elevations can be quantified, providing a measure of the DTM's vertical accuracy. Mean Bias Error (MBE) is employed to evaluate the average difference or bias between the DTM elevations and the ground checkpoints. It measures the systematic error present in the DTM, indicating whether there is a consistent overestimation or underestimation. The MBE calculation formula is as follows:

$$MBE = \frac{(\sum (DTM - Ground))}{n}$$

Any systematic bias in the DTM can be determined by calculating MBE, and its reliability for various applications can be assessed. Correlation Coefficient (CC) is a statistical metric quantifying the linear relationship between the DTM elevations and the ground checkpoints. It measures the strength and direction of the relationship, ranging from -1 to +1. CC can be calculated using various methods, such as Pearson's or Spearman's rank correlation coefficient. By analyzing the CC, we can assess the level of agreement and correlation between the DTM and the ground truth elevations.

2.4.2 Qualitative Assessment

In addition to quantitative metrics, a qualitative assessment is essential to evaluate the visual accuracy and overall quality of the generated DTMs (Figure 13). This section visually compares the six different DTMs with the corresponding orthophoto of the study area. This visual assessment allows for a more intuitive understanding of the performance and suitability of each DTM.

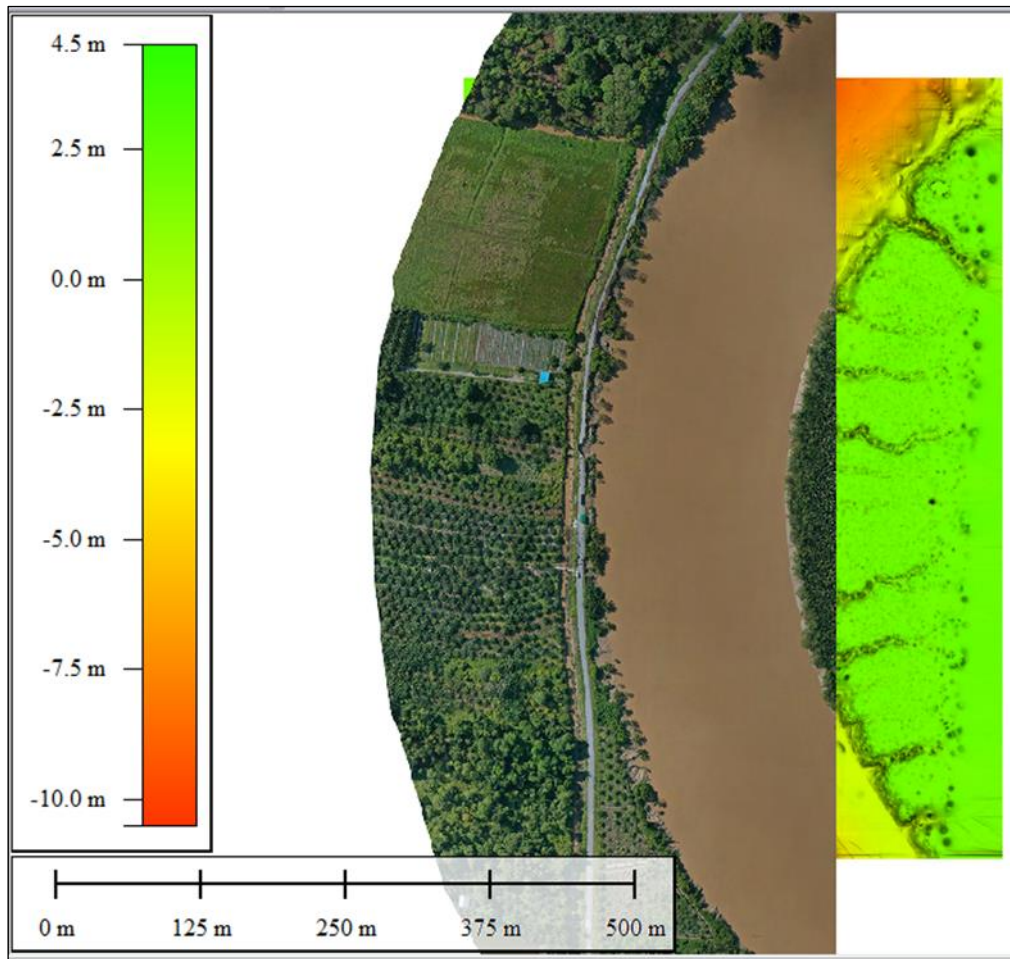


Figure 13. Qualitative assessment between generated DTM and orthophoto via side feature in global mapper

3.0 Results and Discussion

The results for each method were presented individually, and their respective accuracies will be explained in detail. Additionally, 3D plots of the generated DTMs are included to visualize the terrain representation. DTMs in these studies were generated using different UAV Lidar and SBES data densities. What makes this DTM unique compared to others is the integration of these two methods, which is novel in the geoscience community. Figures 14 to 19 show six DTM models generated in 3D plots.

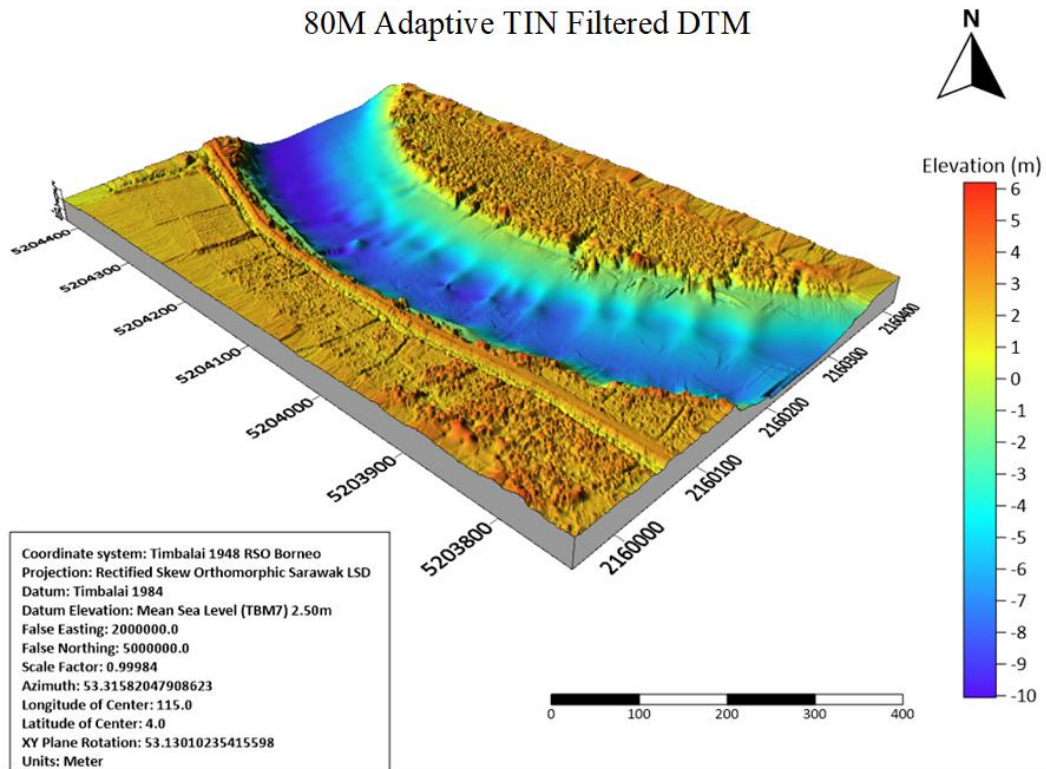


Figure 14. 3D plot of ATIN filtering at 80m flight height

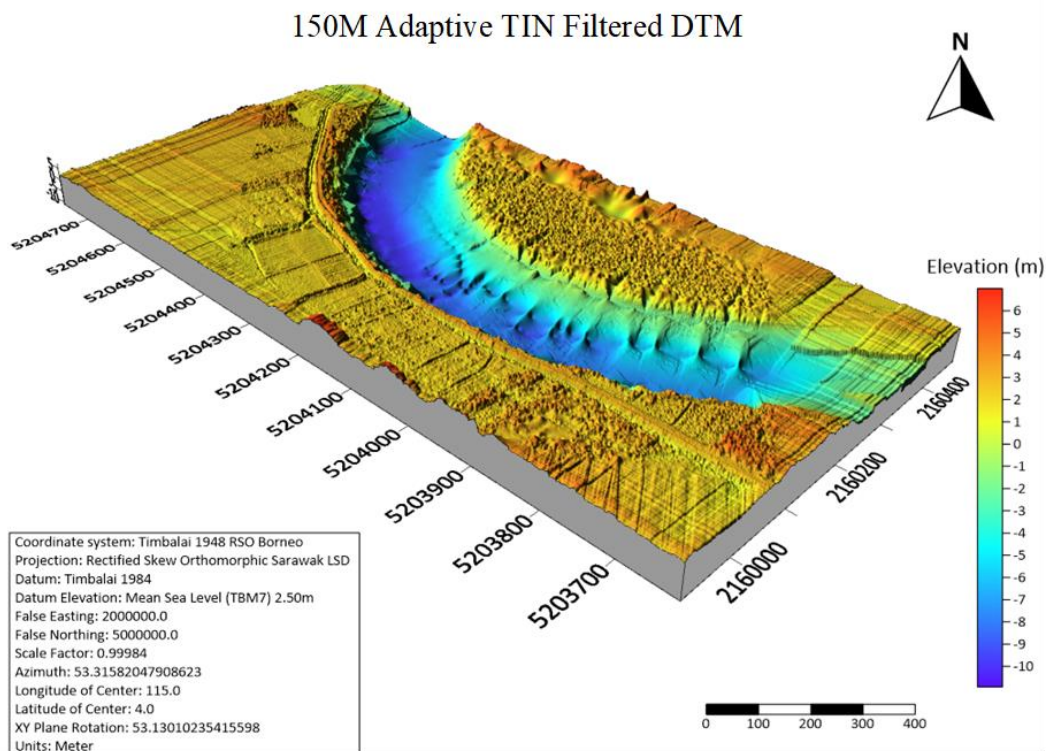


Figure 15. 3D plot of ATIN filtering at 150m flight height

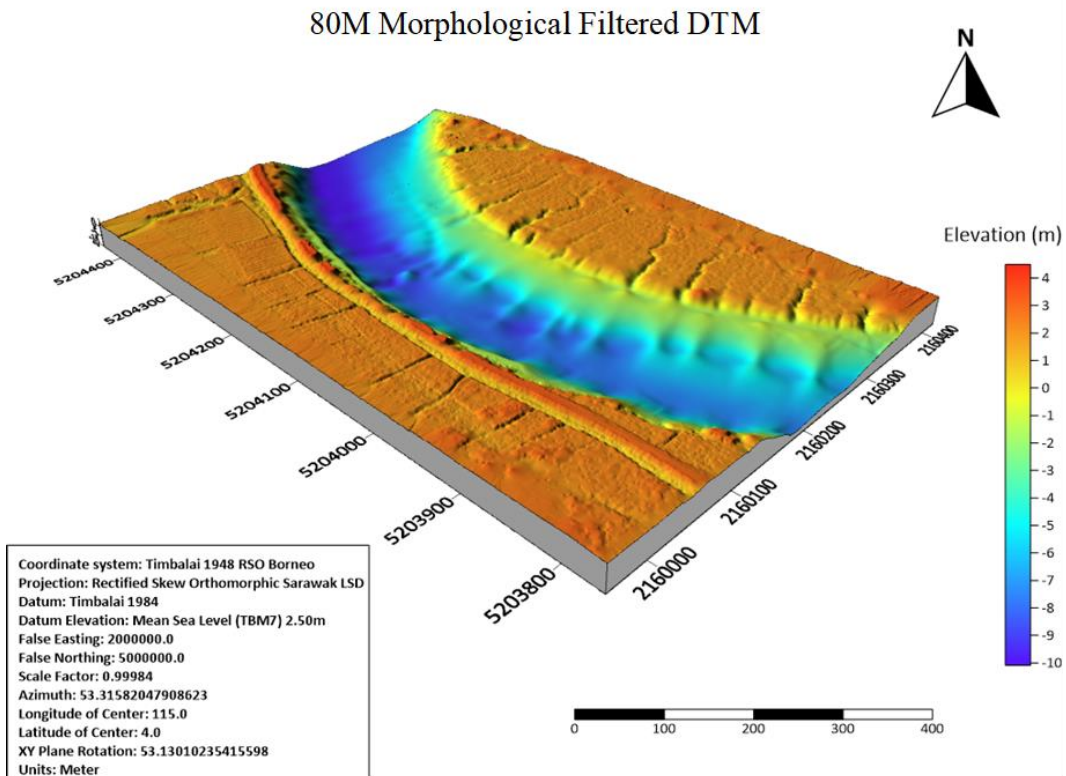


Figure 16. 3D plot of morphological filtering at 80m flight height

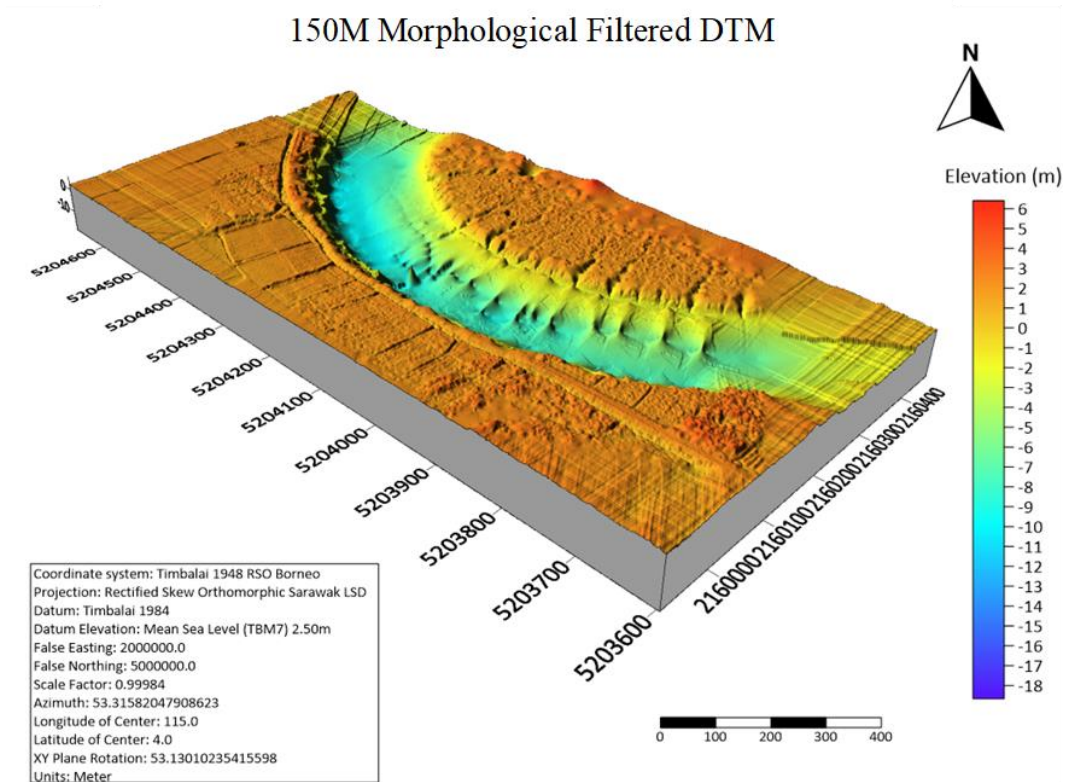


Figure 17. 3D plot of morphological filtering at 150m flight height

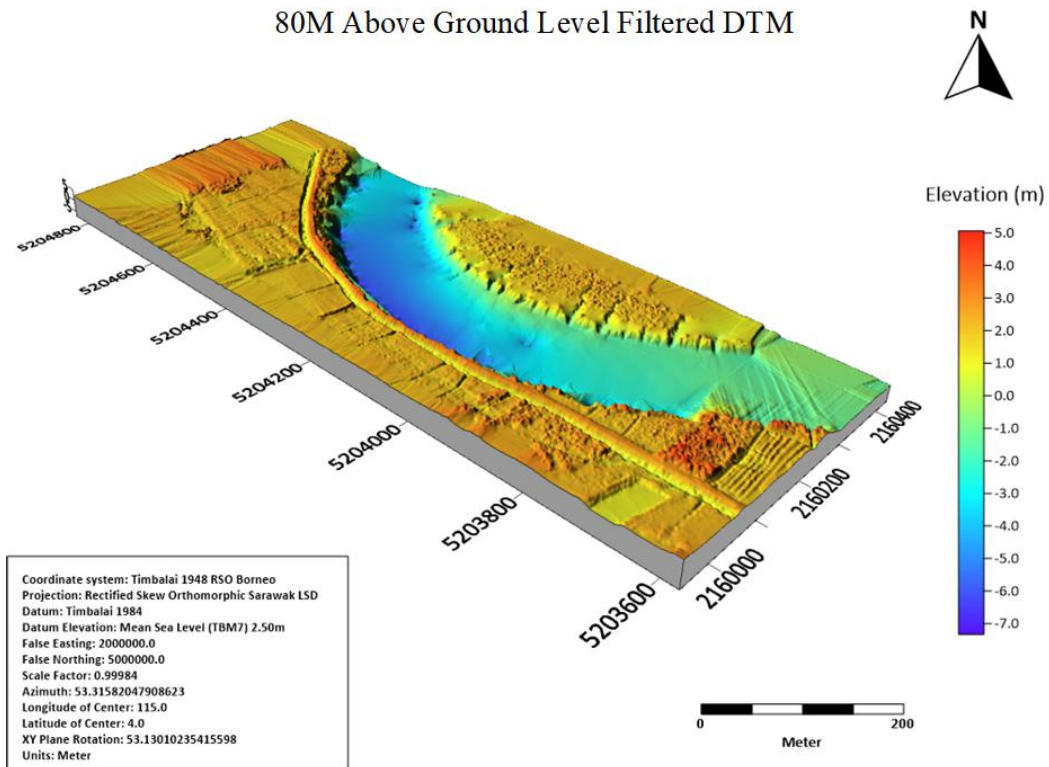


Figure 18. 3D plot of AGL filtering at 80m flight height

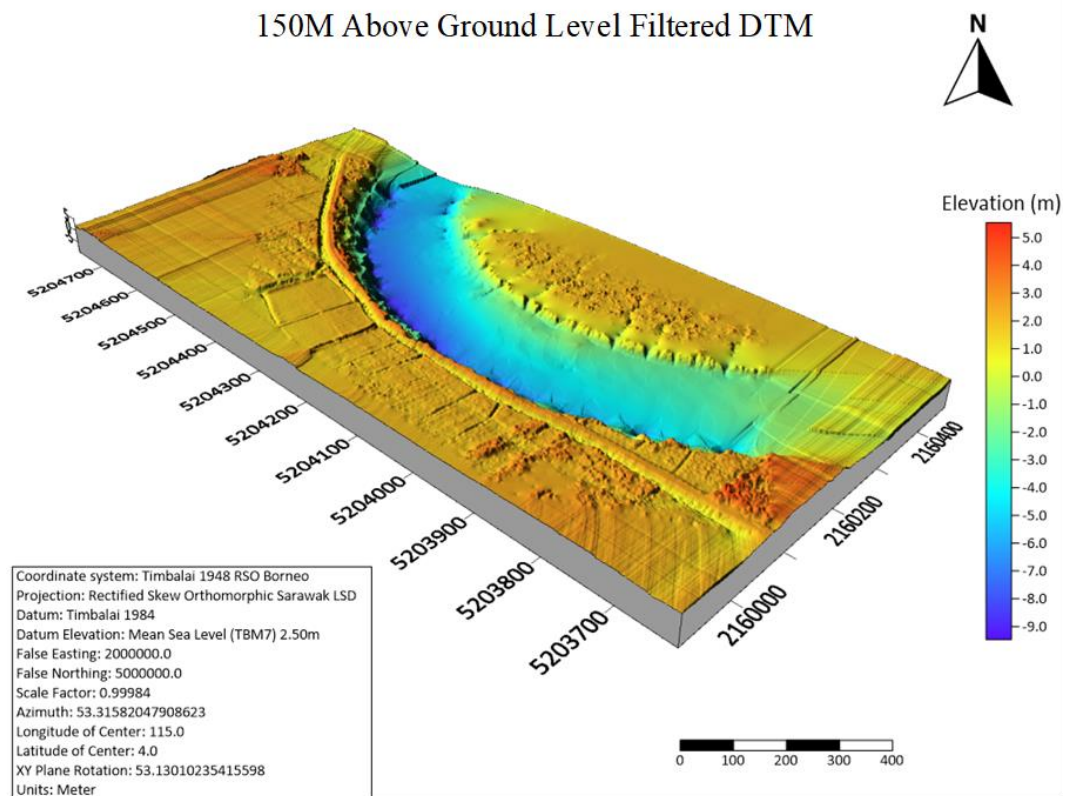


Figure 19. 3D plot of AGL filtering at 150m flight height

3.1 Quantitative Assessment

In this section, the accuracy of the generated DTMs was assessed by evaluating the RMSE metric. The RMSE measures the average vertical deviation between the generated DTM and the reference data, with lower values indicating higher accuracy in representing the terrain characteristics.

Table 2. RMSE results for different data/analysis combinations

| Data/Analysis | RMSE (m) |
|----------------------|-----------------|
| 150Morph_K | 0.23 |
| 80Morph_KR | 0.32 |
| 150ATIN_KR | 0.26 |
| 80ATIN_KR | 0.18 |
| 150AGL_KR | 0.39 |
| 80AGL_KR | 0.30 |

Based on Table 2, the best result in terms of RMSE was observed for the 80ATIN_KR analysis, with an RMSE value of 0.18m. This result indicates a relatively low average vertical deviation between the generated DTM and the reference data, suggesting a high level of accuracy in representing the terrain features. On the other hand, the 150AGL_KR analysis exhibited the highest RMSE value of 0.39m, indicating a slightly higher average vertical deviation compared to the different data/analysis combinations. The variation in RMSE values can be attributed to factors such as the choice of ground filtering methods, flight heights, and the specific terrain characteristics being analyzed. Despite some variations, all the RMSE values fall within an acceptable range, indicating accurate DTMs. Next is the MSE, as tabulated in Table 3.

Table 3. Analysis of MSE

| Data/Analysis | MSE (m) |
|----------------------|----------------|
| 150Morph_K | 0.05 |
| 80Morph_KR | 0.10 |
| 150ATIN_KR | 0.07 |
| 80ATIN_KR | 0.03 |
| 150AGL_KR | 0.16 |
| 80AGL_KR | 0.009 |

The table above summarizes the MSE values obtained for each filtering method. Among the results, the 80ATIN_KR filtering method achieved the lowest MSE value of 0.03m, indicating high accuracy in capturing the elevation values. Conversely, the 80AGL_KR filtering method exhibited the highest MSE value of 1.63m, suggesting a higher deviation between the generated DTM and the reference data. The superior performance of the 80ATIN_KR result, characterized by its lower MSE value, can be attributed to its effective filtering algorithm and optimized parameter selection. On the other hand, the higher MSE value observed for the 80AGL_KR result may stem from factors such as noise in the data, suboptimal filtering parameters, or limitations of the filtering algorithm employed. The Mean Absolute Error (MAE) is another important evaluation metric for DTMs, quantifying the average absolute difference between the elevation values of the generated DTM and the reference data. It provides insights into the overall accuracy and precision of the models.

Table 4. Analysis of MAE

| Data/Analysis | MAE (m) |
|----------------------|----------------|
| 150Morph_K | 0.19 |
| 80Morph_KR | 0.31 |
| 150ATIN_KR | 0.25 |
| 80ATIN_KR | 0.17 |
| 150AGL_KR | 0.38 |
| 80AGL_KR | 0.30 |

The table above presents the MAE values obtained for each filtering method. Notably, the 80ATIN_KR filtering method achieved the lowest MAE value of 0.17m, indicating higher accuracy in capturing the elevation values. Conversely, the 150AGL_KR filtering method exhibited the highest MAE value of 0.38m, suggesting a higher deviation between the generated DTM and the reference data. The superior performance of the 80ATIN_KR result, characterized by its lower MAE value, can be attributed to its effective filtering algorithm and optimized parameter selection. Conversely, the higher MAE value observed for the 150AGL_KR result may be influenced by various factors, including limitations of the filtering method, suboptimal flight height, or specific characteristics of the river and riparian areas.

The MBE is a metric to assess the systematic bias in the generated DTMs. It measures the average difference between the elevation values of the DTM and the reference data, providing insights into the models' overall accuracy and potential biases.

Table 5. Analysis of MBE

| Data/Analysis | MBE (m) |
|----------------------|----------------|
| 150Morph_K | 9.17 |
| 80morph_KR | 8.51 |
| 150ATIN_KR | 8.77 |
| 80ATIN_KR | 9.06 |
| 150AGL_KR | 8.23 |
| 80AGL_KR | 8.56 |

The table above summarizes the MBE values obtained for each filtering method. The 80morph_KR filtering method achieved the lowest MBE value of 8.51m, indicating a relatively lower systematic bias in capturing the elevation values. On the other hand, the 150Morph_K filtering method exhibited the highest MBE value of 9.17m, suggesting a relatively higher systematic bias between the generated DTM and the reference data. Further analysis and interpretation are required to understand the reasons behind the observed variations in MBE results. Data quality, filtering algorithms, flight height, and terrain characteristics may contribute to the differences observed. These factors should be carefully considered to improve the accuracy and mitigate potential biases in future DTM generation. The last analysis is CC, as tabulated in Table 6.

Table 6. Analysis of CC

| Data/Analysis | CC |
|----------------------|-----------|
| 150Morph_K | 1.00 |
| 80morph_KR | 1.00 |
| 150ATIN_KR | 1.00 |
| 80ATIN_KR | 1.00 |
| 150AGL_KR | 0.99 |
| 80AGL_KR | 1.00 |

The table above presents the CC values obtained for each filtering method. Notably, most filtering methods achieved a strong correlation (CC value of 1.00) between the generated DTM and the reference data, indicating a high level of consistency. The 150AGL_KR filtering method exhibited a slightly lower CC value of 0.99, suggesting a strong correlation but with a minor deviation from perfect linearity. The high CC values observed for most filtering methods indicate the accuracy and reliability of the generated DTMs in capturing the elevation values of

the river and riparian areas. However, the slightly lower CC value for the 150AGL_KR result may be attributed to factors such as noise in the data, suboptimal filtering parameters, or variations in the terrain characteristics.

3.2 Qualitative Assessment

This section conducted a qualitative analysis to assess the visual quality and suitability of six different Digital Terrain Models (DTMs), as shown in Table 7.

Table 7: Qualitative Assessment

| Ranking | DTM Filtering Method | Visual Assessment |
|---------|-------------------------------|-------------------------------------|
| 1 | 80m Morphological (Morph) | Excellent alignment with orthophoto |
| 2 | 80m ATIN | Good representation of terrain |
| 3 | 150m Morphological (Morph) | Satisfactory representation |
| 4 | 150m ATIN | Noticeable discrepancies |
| 5 | 80m Above Ground Level (AGL) | Inconsistencies with orthophoto |
| 6 | 150m Above Ground Level (AGL) | Discrepancies with orthophoto |

3.3 Optimum Result Based on Accuracy Assessment

This section analyzed the overall analysis of the DTMs generated for river and riparian areas using different filtering methods. The study aims to evaluate the accuracy and performance of the six DTMs by comparing the results obtained from various analysis metrics, including RMSE, MSE, MAE, MBE, CC and visual assessment.

Table 8: Summary of Analysis Results and Overall Ranking of Filtering Method

| Overall Ranking | DTM Filtering Method |
|-----------------|-------------------------------|
| 1 | 80m ATIN |
| 2 | 80m Morphological (Morph) |
| 3 | 150m Morphological (Morph) |
| 4 | 150m ATIN |
| 5 | 80m Above Ground Level (AGL) |
| 6 | 150m Above Ground Level (AGL) |

Based on Table 8, the overall findings indicate that the 80m ATIN filtering method exhibited superior performance to the other methods evaluated. This suggests that adaptive filtering algorithms like ATIN can extract ground points and produce accurate DTMs in these environments. One key aspect that contributed to the success of the 80m ATIN method is the flight height. The 80-meter flight height proved to be more suitable for capturing detailed terrain features and achieving higher accuracy than the 150-meter flight height. This finding highlights the importance of carefully considering flight parameters during data acquisition to optimize DTM generation in river and riparian areas.

The observed performance variations among the filtering methods can be attributed to their underlying principles and algorithms. Morphological filtering methods consider the terrain characteristics and shape, such as the 80m Morph and 150m Morph. While these methods generally performed well in terms of accuracy, they may encounter limitations in capturing complex terrain features accurately, leading to slightly higher errors. On the other hand, the ATIN filtering methods, including the 80m ATIN and 150m ATIN, demonstrated strong performance in terms of accuracy measures. These methods utilize adaptive algorithms that account for specific flight altitudes, allowing for more precise ground point extraction and DTM generation. The ATIN approach effectively captured terrain details and produced accurate DTMs in river and riparian areas.

It is important to acknowledge that the accuracy of the generated DTMs is influenced by various factors beyond the filtering methods, including the quality of the input data, data processing techniques, and environmental conditions. Further refinements in data acquisition techniques, such as improving the resolution and density of the input data and advancements in filtering algorithms, could potentially enhance the accuracy and reliability of DTMs in these environments.

4.0 Conclusion and Recommendation

The study focused on the accuracy and alignment of the DTM with reference data. Among the methods evaluated, the 80m ATIN filtering method exhibited the highest overall accuracy, demonstrating excellent alignment with the orthophoto. The 150m ATIN method showed noticeable discrepancies and lower accuracy. The 80m Morphological method outperformed the 150m Morphological method but still had slightly higher errors than the 80m ATIN method. The 80m AGL method displayed inconsistencies and lower accuracy, as did the 150m AGL method. The generated DTMs hold significant value for government agencies involved in land

management, environmental monitoring, and flood risk assessment. They can support decision-making processes, infrastructure planning, and environmental management strategies.

Despite the positive outcomes, certain limitations should be acknowledged. The study used data from only two flight heights, and expanding the dataset to include more altitudes or densities would improve generalizability. Additionally, the research solely relied on an SBES for data collection, and future studies should consider incorporating multi-beam echo sounder (MBES) data to enhance coverage and accuracy. The research also used kriging as the interpolation method. However, exploring alternative methods like inverse distance weighting or spline interpolation can provide insights into their suitability for DTMs in river and riparian areas.

Several recommendations for future studies are proposed based on the findings and limitations. These include incorporating data from various altitudes or densities, exploring the use of MBES for improved coverage, and investigating alternative interpolation methods to refine the accuracy of DTMs. By considering these recommendations, future research can enhance the understanding and construction of DTMs in river and riparian environments.

Acknowledgement

The authors would like to thank the Ministry of Higher Education and the Universiti Teknologi Malaysia for providing financial support under the Fundamental Research Grant Scheme (FRGS) FRGS/1/2020/TK02/UTM/02/1 (UTM vote No. R.J130000.7852.5F396).

References

- Abdul Rahman, A. (1994). Digital Terrain Model Data Structures. *Buletin Ukur*, (1), 61–66. Retrieved from <http://eprints.utm.my/4977/>
- Abdullah, A., Rahman, A., & Vojinovic, Z. (2009). LiDAR filtering algorithms for urban flood application: Review on current algorithms and filters test. *International Archives of Photogrammetry, Remote Sensing and Spatial Information Sciences*, XXXVIII (Part 3), 30–36.
- Akihisa, W., Toshiaki, Y., Masaaki, M., Takanari, A., Hideo, A., & Hirokazu, T. (2011). A Surveillance System Using Small Unmanned Aerial Vehicle (UAV) Related Technologies. *NEC Technical Journal*, 8(1), 68–73.
- Axelsson, P. (2000). DEM Generation from Laser Scanner Data Using Adaptive TIN Models. *International Archives of Photogrammetry and Remote Sensing*, 33(Part B4), 110–117. <http://doi.org/10.1016/j.isprsjprs.2005.10.005>

- Bachrach, A., Prentice, S., & Roy, N. (2011). RANGE - Robust Autonomous Navigation in GPS-denied Environments.
- Briese, C. (2010). Extraction of digital terrain models. In G. Vosselman, and H. Maas (Eds.), *Airborne and Terrestrial Laser Scanning*. Dunbeath: Whittles Publishing. pp. 147-150
- Chisholm, R. A., Cui, J., Lum, S. K. Y., & Chen, B. M. (2013). UAV LiDAR for below-canopy forest surveys. *Journal of Unmanned Vehicle Systems*, 01(01), 61–68.
- Dandois, J. P., Olano, M., & Ellis, E. C. (2015). Optimal Altitude, Overlap, and Weather Conditions for Computer Vision UAV Estimates of Forest Structure, 13895–13920.
- Darwin, N., Ahmad, A., Amin, Z. M., & Zainon, O. (2014). *Jurnal Teknologi Full Paper Assessment of Photogrammetric Micro Fixed-Wing Unmanned Aerial Vehicle (UAV) System for Image Acquisition of Coastal Area*, 5, 31–36.
- Lin, Y., Hyypää, J., & Jaakkola, A. (2011). Mini-UAV-borne LIDAR for fine-scale mapping. *IEEE Geoscience and Remote Sensing Letters*, 8(3), 426–430.
- Maguya, A. S., Junttila, V., & Kauranne, T. (2014). Algorithm for extracting digital terrain models under forest canopy from airborne LiDAR data. *Remote Sensing*, 6(7), 6524–6548.
- Meng, X., Currit, N., & Zhao, K. (2010). Ground filtering algorithms for airborne LiDAR data: A review of critical issues. *Remote Sensing*, 2(3), 833–860.
- Meng, X., Wang, L., Silván-Cárdenas, J. L., & Currit, N. (2009). A multi-directional ground filtering algorithm for airborne LIDAR. *ISPRS Journal of Photogrammetry and Remote Sensing*, 64(1), 117–124.
- Nedjati, A., Vizvari, B., & Izbirak, G. (2015). Post-earthquake response by small UAV helicopters. *Natural Hazards*, 80(3), 1669–1688.
- Zhang, K., & Whitman, D. (2005). Comparison of Three Algorithms for Filtering Airborne Lidar Data. *Expert Systems with Applications*, 24(4), 433–441.
- Zhang, K., Cui, Z., & Hurricane, I. (2007). *Airborne LIDAR Data Processing and Analysis Tools*. Data Processing, (April).